European Journal of Cancer 217 (2025) 115252

Contents lists available at ScienceDirect

European Journal of Cancer

journal homepage: www.ejcancer.com

Reduced monocytic IL10 expression in PD1 inhibitor-treated patients is a harbinger of severe immune-related adverse events

Stanislav Rosnev [a,b], Baldur Sterner [a,b], Phillip Schiele [a,b], Stefan Kolling [a,b,c], Markus Martin [a], Anne Flörcken [a,d], Barbara Erber [e], Friedrich Wittenbecher [a,f], Grzegorz Kofla [a], Annika Kurreck [a], Tonio Johannes Lukas Lang [a], Jobst C. von Einem [a], Maria de Santis [e,g], Uwe Pelzer [a], Sebastian Stintzing [a], Lars Bullinger [a,d], Konrad Klinghammer [a,h], Dominik Geisel [i], Sebastian Ochsenreither [a,d,h], Marco Frentsch [a,b,h,1], Il-Kang Na [a,d,f,j,*,1]

[a] Department of Hematology, Oncology and Cancer Immunology, Charité-Universitätsmedizin Berlin, Corporate Member of Freie Universität Berlin, Humboldt-Universität zu Berlin, and Berlin Institute of Health, Berlin, Germany
[b] Berlin Institute of Health Center for Regenerative Therapies, Charité-Universitätsmedizin Berlin, Corporate Member of Freie Universität Berlin, Humboldt-Universität zu Berlin, and Berlin Institute of Health Berlin, Germany
[c] Berlin School of Integrative Oncology, Berlin, Germany
[d] German Cancer Consortium (DKTK), Berlin, Germany
[e] Department of Urology, Charité-Universitätsmedizin Berlin, Corporate Member of Freie Universität Berlin, Humboldt-Universität zu Berlin, and Berlin Institute of Health, Berlin, Germany
[f] Berlin Institute of Health (BIH), Berlin, Germany
[g] Department of Urology, Medical University of Vienna, Vienna, Austria
[h] Charité Comprehensive Cancer Center, Charité-Universitätsmedizin Berlin, Corporate Member of Freie Universität Berlin, Humboldt-Universität zu Berlin, and Berlin Institute of Health, Berlin, Germany
[i] Department of Radiology, Campus Virchow-Klinikum, Charité-Universitätsmedizin Berlin, Corporate Member of Freie Universität Berlin, Humboldt-Universität zu Berlin, and Berlin Institute of Health, Berlin, Germany
[j] Experimental and Clinical Research Center, A Cooperation of Charité-Universitätsmedizin Berlin and Max Delbrück Center for Molecular Medicine, Berlin, Germany

ARTICLE INFO

Keywords:
Cancer immunotherapy
Immune checkpoint blockade
PD1
Immune-related adverse events
Biomarkers
Monocytes
IL10

ABSTRACT

Background: Despite remarkable clinical efficacy, little is known about the system-wide immunological alterations provoked by PD1 blockade. Dynamics of quantitative immune composition and functional repertoire during PD1 blockade could delineate cohort-specific patterns of treatment response and therapy-induced toxicity.

Methods: We longitudinally assessed therapy-induced effects on the immune system in fresh whole blood using flow cytometry-based cell quantifications, accompanied by analyses of effector properties of all major immune populations upon cell-type specific stimulations. 43 cancer patients undergoing PD1 blockade were recruited with assessments performed pre-treatment and before cycles 2/4/6, which resulted in the collection of more than 30,000 cytometric data values.

Results: We observed no intrinsic immune pattern correlating with clinical outcome before PD1 blockade initiation, but cohort-specific immune alterations emerged during therapy. The most striking evolving changes in therapy responders were an increase in activated T and NK cell subsets, which showed high IFNγ and TNFα expression upon ex vivo stimulation. Patients affected by severe immune-related adverse events (s-irAE) presented with an analogously increased number of activated $CD4^+$ and $CD8^+$ T cells compared to patients with no/mild irAE, but lacked the functional divergences observed between responders versus non-responders. Instead, their monocytes showed discriminatory functional deficits with less IL10 production upon

* Corresponding author at: Department of Hematology, Oncology and Cancer Immunology, Charité-Universitätsmedizin Berlin, Corporate Member of Freie Universität Berlin, Humboldt-Universität zu Berlin, and Berlin Institute of Health, Berlin, Germany.
E-mail address: il-kang.na@bih-charite.de (I.-K. Na).
[1] These authors supervised the study.

https://doi.org/10.1016/j.ejca.2025.115252
Received 29 August 2024; Received in revised form 11 January 2025; Accepted 16 January 2025
Available online 17 January 2025

stimulation, which led to an abrogated inhibition of T cell proliferation in vitro and thus may account for the observed T cell expansion in patients with s-irAE.
Conclusion: Our holistic explorative approach allowed the delineation of clinically relevant cohorts by treatment-triggered immune changes, potentially enabling better patient stratification and further revealed new mechanistic insights into the pathogenesis of s-irAE.

1. Introduction

Immune checkpoint blockade (ICB) can achieve remarkable long-term responses [1,2]; however, a significant group of patients does not benefit from ICB treatment due to primary resistance or becoming resistant following initial response [3]. A second major challenge for the successful application of ICB is the occurrence of treatment-induced autoimmune toxicities directed against non-malignant tissues. Patients undergoing anti-PD1/PDL1 therapy are reported to develop immune-related adverse events (irAE) with severe and life-threatening irAE observed in 15–20 % of patients [4–6]. The cumulative number of irAE is constantly increasing due to approvals of ICB for additional indications and as combination treatment. IrAE can affect any organ system and can show erratic kinetics of appearance.

Our understanding of the underlying mechanisms of action of ICB in the context of PD1/PDL1 blockade is still incomplete. Coordinated interactions across various leukocyte populations and multiple tissues accompanied by immune activation in the periphery seem to be a crucial prerequisite for the initiation of effective ICB-triggered anti-tumor reactions [7,8]. In addition to re-activation and rejuvenation of pre-existing terminally differentiated or 'exhausted' tumor-infiltrating lymphocytes (TILs) [9], PD1 blockade may also lead to expansion of novel T cell clonotypes from tumor-extrinsic sources and clonal replacement of tumor-specific TILs [10]. Such peripherally expanded clones, also detectable in peripheral blood from patients [11,12], indicate the importance of system-wide off-TME effects of ICB in explaining the highly variable clinical outcomes in patients including treatment response/failure as well as development and severity of irAE. To date, the role of myeloid lineage cells in the context of PD1/PDL1 blockade has been underappreciated, but recently emerged as a key element in tumor growth control [13,14] and myeloid cell-specific PD1 ablation was revealed to mediate better antitumor protection than T cell-specific ablation [15]. In addition, consistent with a previous observation that a decrease of IL10 coincides with the onset of irAE in an anti-CTLA4 treated patient [16], Nunez et al. [17] also observed reduced serum IL10 levels as potential indicator of heightened risk of developing irAE.

Peripheral leukocytes in patients undergoing PD1 blockade have been mostly analyzed according to their phenotypical characteristics, which only allows for an imprecise assessment of the effector repertoire and the reactivity of specific immune cell populations and their functional shifts during ICB. We established a flow cytometry-based immune screening platform to quantify the major leukocyte populations in fresh peripheral blood and assess directly ex vivo their functionality upon activation of various cell type-specific signalling pathways. Determining the reactivity of T, B, NK cells, monocytes, and DCs by measuring multiple effector functions, such as expression of activation markers, production of cytokines, and phagocytic activity, upon stimulation with various pre-defined reagents, enabled a more comprehensive analysis of ICB-induced functional alterations. Screening tumor patients prior to treatment and during PD1 blockade allowed us for the first time to assess dynamic changes in the reactive capacity of immune cells (i.e., immune cell function) in the context of quantitative immune cell trends and thereby the immune cellular network. This enabled us to investigate associations between the entirety of quantitative and qualitative immune cell parameters with clinical response and the development of irAE, whereby we focused on severe irAE requiring at least temporary ICB discontinuation and systemic glucocorticoid treatment. The aim of this explorative study was the longitudinal capture of treatment-triggered immune changes for the deeper and improved understanding of the functional mechanisms at play regarding ICB efficacy and autoimmune toxicity. The concrete objectives of these analyses focused on the comparison of baseline characteristics as well as treatment-induced dynamic changes of circulating immune cell populations between responders and non-responders on the one hand and patients developing severe irAEs and those who did not on the other.

2. Materials and methods

2.1. Study design

The study was approved by the Ethics Committee of Charité-Universitätsmedizin Berlin. Informed consent from all study participants was obtained regarding the prospective blood sampling and review of clinical data. In total 43 patients with head and neck squamous cell carcinoma (HNSCC), renal cell carcinoma (RCC), non-small cell lung cancer (NSCLC), carcinoma of unknown primary (CUP), melanoma, urothelial carcinoma, or colon cancer undergoing anti-PD1 treatment at our institution were recruited to the study between January 2019 and April 2021. The general and individual clinical characteristics of the study cohort are summarized in Table 1 and Tab. S1. Only ICB therapy-naïve patients were included. Peripheral blood samples from patients were collected once before the initiation of ICB treatment (C1) and three times during treatment, before the 2nd (C2), 4th (C4), and 6th (C6) application of therapy according to the drug-dependent dosing schemes. Additionally, nine healthy individuals were added to the study as an age-matched control group. In a similar manner blood samples from the healthy controls were obtained at four time points in a two-week cycle. Symptoms of acute infection at the moment of blood sampling were ruled out. Data on the incidence, timing, and management of irAE in the ICB-treated patients were collected. The irAE development and the required immunosuppressive treatment regimens were documented by the treating physicians and graded according to the National Cancer Institute's Common Terminology Criteria for Adverse Events (CTCAE; version 5.0). A summary of the irAE observed in our study cohort is presented in Tab. S4. Observed irAE were classified as severe in the case of CTCAE grade > 2 requiring at least temporary ICB discontinuation and application of high-dose systemic steroids. Initial treatment response was determined in accordance with iRECIST criteria [18] and clinical assessment between week 8 and 16 of ICB treatment. "Responders" (R) were defined as patients with stable disease, complete, or partial response regardless of response duration, whereas patients with progressive disease were categorized as "non-responders" (NR). Data on initial treatment response, best overall response, and time to disease progression of the study participants are presented in Tab. S1.

2.2. Antibodies and stimulation reagents

An overview of the applied fluorochrome-conjugated antibodies can be found in Tab. S5. All antibodies were titrated beforehand for optimal staining resolution.

Fresh whole blood samples were stimulated within our functional assay as described below. An overview of the stimulation agents, the applied concentrations, as well as their functions and company details can be found in Tab. S6. The concentration of each stimulation reagent was determined according to previously performed dose–response curves with several concentrations. Brefeldin A (Sigma-Aldrich, USA)

Tab. 1
Overview of general patient characteristics. Information about sex, age, tumor type, PD1 blockade therapy as monotherapy or combination treatment, prior therapies, current line of treatment, as well as observed irAE and initial treatment response according to iRECIST criteria [22] and clinical assessment by week 16 upon treatment initiation is presented in the table.

	Number	%
Sex		
Male	33	76.7
Female	10	23.3
Age		
≤ 50	6	14.0
50–70	23	53.4
≥ 70	14	32.6
Tumour Type		
HNSCC	20	46.5
RCC	13	30.2
NSCLC	4	9.3
Other (CUP, melanoma, urothelial/colon carcinoma)	6	14.0
Therapy		
Nivolumab	23	53.5
Pembrolizumab	12	27.9
Ipilimumab/Nivolumab	4	9.3
Pembrolizumab/Chemotherapy	3	7.0
Pembrolizumab/TKI	1	2.3
Prior Radiotherapy		
Yes	18	41.9
No	25	58.1
Prior Chemotherapy		
Yes	17	39.5
No	26	60.5
Prior TKI		
Yes	11	25.6
No	32	74.4
Prior EGFR Inhibitors		
Yes	10	23.3
No	33	76.7
Number of Prior Treatment Regimens		
0	14	32.6
1	13	30.2
2	13	30.2
3	3	7.0
Severe irAE (> Grade 2)		
Yes	8	18.6
No	35	81.4
Number of Severe irAE (> Grade 2)		
0	35	81.4
1	6	14.0
2	1	2.3
≥3	1	2.3
Initial Treatment Response		
Complete Response	0	0.0
Partial Response	17	39.6
Stable Disease	4	9.3
Progressive Disease	22	51.1

was used for the intracellular staining in the functional assay (Fig. S3) as a blocker of protein secretion as described below.

2.3. Flow cytometry of major immune cell populations and subpopulations

Two samples of 100 µl fresh heparinized whole blood were directly stained with either 18 fluorochrome-conjugated antibodies for the quantification of the major blood leukocyte populations or 11 fluorochrome-conjugated antibodies for the quantification of T cell subpopulations. The staining was performed in darkness at room temperature for 15 min. Afterwards 1 ml of erythrocyte lysis buffer (Qiagen, Germany) was added, and the samples were incubated for another 30 min in darkness on ice with intermittent vortexing. After 30 min 900 µl of PBS + 0.2 % BSA were added, and the samples were immediately measured using a CytoFLEX LX cytometer (Beckman Coulter, USA). Instrument performance was monitored daily with CytoFLEX daily QC fluorospheres (Beckman Coulter, USA). A defined volume of 500 µl per sample was measured, allowing for calculation of cells per µl whole blood. Flow cytometry data was analyzed using CytExpert Software Version 2.4 (Beckman Coulter, USA). Evaluated cell populations are summarized in Tab. S2/S3 and the applied gating schemes are shown in Fig. S1A-B.

2.4. Flow cytometric assessment of immune cell functions

300 µl of fresh heparinized whole blood was used per stimulation sample. According to manufacturer's instructions of the DurActive 1 stimulation tubes from Beckman Coulter, the PI stimulation was performed with only 50 µl of whole blood. The monocytes and DCs stimulation samples (see Fig. S3) as well as the PI (PMA/ionomycin) stimulation sample for T cells were cultured for 4 h at 37°C in the presence of 20 µg/ml brefeldin A (Sigma-Aldrich, USA). All other samples were stimulated for 22 h at 37°C and brefeldin A was added 3 h after stimulation start. 30 ng/ml phorbol-12-myristat-13-acetat (PMA) and 1 µg/ml ionomycin (Sigma-Aldrich, USA) were added 4 h before the end of the stimulation period into all whole blood B-cell stimulation samples as well as the corresponding control sample as an efficient B-cell trigger.

After the stimulation period 3 ml of erythrocyte lysis buffer (Qiagen, Germany) were added and the samples were incubated for 20 min in darkness on ice with intermittent vortexing. Next, cells were washed with PBS and staining of surface antigens was carried out for 10 min in the presence of 1 mg/ml beriglobin (Sanofi, France). To exclude dead cells, aqua fluorescent reactive dye (Invitrogen, USA) was added together with one of four cell-type specific antibody mixes for T cells, B cells, NK cells, and monocytes plus DCs. Fixation and permeabilization were performed with IC (intracellular) fixation and permeabilization buffer (Invitrogen, USA) according to the manufacturer's protocol and intracellular staining was carried out in the presence of beriglobin for 25 min in the dark at room temperature with one of the four cell-type specific antibody mixes (Fig. S3). Samples were measured on a CytoFLEX LX cytometer (Beckman Coulter, USA) and analyzed by using CytExpert Software Version 2.4. Evaluated immune functions are summarized in Fig. S3 and the applied gating scheme for all four antibody panels is shown in Fig. S1C-G.

2.5. IL10 ELISA

IL10 levels in ICB patient sera pre- and on-treatment diluted 1:1 in PBS were assessed using the Human IL-10 ELISA Kit (RayBiotech, USA) according to the manufacture's protocol. In order to detect IL10 produced by monocytes of irAE and n-irAE patients, $CD14^+$ monocytes were isolated from PBMCs by positive selection using the EasySep human CD14 Positive Selection Kit II (Stemcell Technologies, Canada) and cultivated for 24 h in RPMI (Thermo Fisher, Germany) supplemented with 5 % human Ab serum (PAN-Biotech, Germany) and 1 % penicillin/streptomycin (Sigma Aldrich, USA). Afterwards, secreted IL10 in the cell culture was analyzed by ELISA MAX Deluxe Set human IL-10 (Biolegend, USA).

2.6. T cell proliferation assay

Supernatant from $CD14^+$ monocytes of irAE and n-irAE ICB patients was generated after isolation and 24 h incubation as described previously. On the next day, autologous PBMCs were labeled with 0.5 µM CFSE (Biolegend, USA) and stimulated with 2.5 µg peptide/ml CEFX Ultra SuperStim Pool (JPT, Germany) and 1 µg/ml αCD28 in the presence or absence of 1:3 diluted monocyte supernatant. After 4 d incubation, proliferation of $CD8^+$ T cells was analyzed by flow cytometry.

2.7. Data analysis and statistics

Flow cytometry data analysis was performed using R (v.4.0.0)

including the following packages tidyverse, reshape2, ggrepel, ggpubr, gridExtra, scales, Rtsne, pheatmap, viridis, RColorBrewer, survival, survminer, sjPlot, enrichplot, and clusterProfiler.

In stimulation experiments, frequencies of activated immune cells were background-corrected using unstimulated control samples.

Due to the high coefficient of correlation between CD3, CD4, and CD8 cell counts observed in the whole blood leukocyte and T cell FACS panels (Fig. S2), the mean of these values was calculated to simplify further analysis.

Parameters were removed 1) in case of a relative coefficient of variance above 0.1 in one of two experiments performed in quadruplicate or 2) in case of a higher averaged intra-visit variance in the healthy controls (HC) compared to the ICB patients (Fig. S4).

To obtain information on the longitudinal alterations induced by successive ICB antibody administrations, the longitudinal data were condensed into a single value (slope) by calculating the median of the three time points during therapy for each parameter and subtracting this median from the pre-treatment value. These integrated values (abbreviated as delta-median or Δ median) represented the longitudinal slope of each parameter, thus showing either increase or decrease of the specific parameter during therapy.

In several analyses, certain related functional parameters were pooled by averaging z-score standardized values of the major immune cell populations with the same effector read out or with the same stimulation (Fig. S3). In this way, we were able to assess the general therapy-induced changes in the responsiveness of defined leukocyte populations to a specific stimulus on the one hand (e.g., PI, LPS) and the general therapy effect on certain effector functions such as TNFα or IL10 production on the other.

Apart from the analysis of the components of variance, for all the statistical analyses non-parametric tests were used as specifically mentioned in the figure legends, since more than half of the tested parameters appeared to not be normally distributed as tested by the Shapiro-Wilk's method. Except for GSEA, adjustment for multiple testing was not performed to avoid higher risk for false negatives (type II errors), while accepting an increased risk for false positives (type I errors) in such an explorative study [19]. Generally, false negatives (type II errors) massively increase by adjustments for multiple testing if the number of parameters is substantially higher than the number of donors ($p >> N$) and if a less powerful non-parametric test has to be chosen. The only test in which we used parametric ANOVA test was for the calculation of the components of variance due to absence of alternative applicable non-parametric methods to calculate the variance distributions. For simplification, we performed the explorative analysis for all parameters including the non-normally distributed parameters to obtain a general impression of the differences between count and functional parameters regarding inter-individual vs. intra-individual inter-visit variance.

We employed the principles of GSEA to determine the therapy duration with the biggest system-wide immune differences between R and NR, as well as irAE and non-irAE. To do so, the differences between all three on-treatment measurements (C2, C4, C6) and the pre-treatment baseline (C1) were calculated for each count and pooled functional parameter. As a next step for all three parameter-specific delta values (C2ΔC1, C4ΔC1, C6ΔC1) a Wilcoxon signed rank test was performed. Finally, all obtained p values were ranked and the weighted Kolmogorov–Smirnov statistic/test was performed by using the elapsed therapy time sets (C2ΔC1, C4ΔC1, C6ΔC1) instead of gene sets in the analysis. In contrast to other statistical tests, here we adjusted the p value by the false discovery rate, since in this setting the number of variable sets was very low compared to the number of ranks.

3. Results

3.1. An immune screening platform allows for assessment of 46 cell count and 81 functional whole blood parameters per time point

To assess the dynamic alterations of immune responses to PD1 blockade, we collected blood from patients undergoing ICB in a longitudinal manner – one pre-treatment (C1), and three on-treatment samples, before the second (C2), forth (C4), and sixth (C6) administration (Figure 1). In total, 43 patients treated with PD1 inhibitors (nivolumab or pembrolizumab) were included in the study (Table 1/S1).

Therapy-induced changes were quantified longitudinally in fresh whole blood samples using two phenotypic panels (Tab. S2/S3). The applied gating hierarchy and the extracted count parameters are summarized in Fig. S1A-S1C and Tab. S2/S3. High coefficients of correlation were observed for parameters (e.g., CD3, CD4, and CD8) measured in parallel by both panels, confirming the robustness of the flow-cytometric assays ($r = 0.96$, $p < 2.2x10^{-16}$; Fig. S2). Additionally, we assessed functional immune shifts during ICB through selected immune cell-type specific physiological stimulations. To minimize possible interference as a consequence of cell preparation, freezing and thawing procedures, we used fresh whole blood samples. Multiple stimulation reagents such as Toll-like receptor (TLR) agonists (R848, LPS, CpG), superantigens (SEB, TSST-1), mitogens (PMA/Ionomycin (PI)), peptide pools, and combinations of cytokines were applied, which enabled the triggering of a wide spectrum of signaling pathways with differing activation strengths and response dynamics (Fig. S3). Subsequent assessment of the responses of T, B, NK, and monocytes plus DCs were performed via four lineage-specific flow-cytometric panels covering activation marker expression, cytokine production, and phagocytotic function (Fig. S3; gating hierarchy Fig. S1D-G).

The initial processing of the acquired data consisted of 52 cell count and 123 functional parameters per time point and patient, resulting in 30,878 data points in total for all enrolled patients. After filtering (see details in Supplementary Methods and Fig. S4) 46 cell count and 81 functional parameters distributed over all immune cell populations were included in the further analysis (Figure 1B).

3.2. The quantitative and functional immune status of cancer patients is already different before ICB treatment compared to healthy controls (HC)

By comparing each parameter between HC and ICB patients at baseline (C1), HC showed significantly higher average lymphocyte blood cell counts, especially for B cells ($p = 0.003$), $CD4^+$ T cells ($p = 0.005$), and their related subsets (Fig. S5A). In contrast, ICB patients displayed significantly higher levels of granulocytes ($p = 0.025$) which mainly stemmed from higher neutrophil counts ($p = 0.003$) compared to HC. To increase the robustness of the functional values and reinforce general trends, related functional parameters were pooled together by averaging the z-score standardized values of functional parameters from a single immune cell population according to the same effector read-out or the same stimulation. In this manner, the pooled functional parameters would sum up a population-specific effector function (e.g., average IL17A expression in $CD4^+$ T cells upon different stimulations; CD4_IL17) or a population-specific response to a certain stimulation (e.g., B cell response to stimulation with ODN; B_ODN). We observed that ICB patients generally responded with higher expression of $CD4^+$ T cell-derived IL17A ($p = 0.002$), monocyte-derived IL10 ($p = 0.016$), and DC-derived IL1β ($p = 0.029$) and that their $CD8^+$ T cells were more reactive to super-antigens ($p = 0.008$; CD8_ST28 [SEB+TSST-1 and αCD28 antibody]) compared to HC (Fig. S5B). In contrast, HC responded with more NK cell-derived IFNγ ($p = 0.011$) and their B cells displayed substantially higher responsiveness to demethylated DNA, ODN ($p = 0.0002$). While not all contributing single functional parameters were significant on their own, there was a universal trend among all parameters of the same functional pool. This

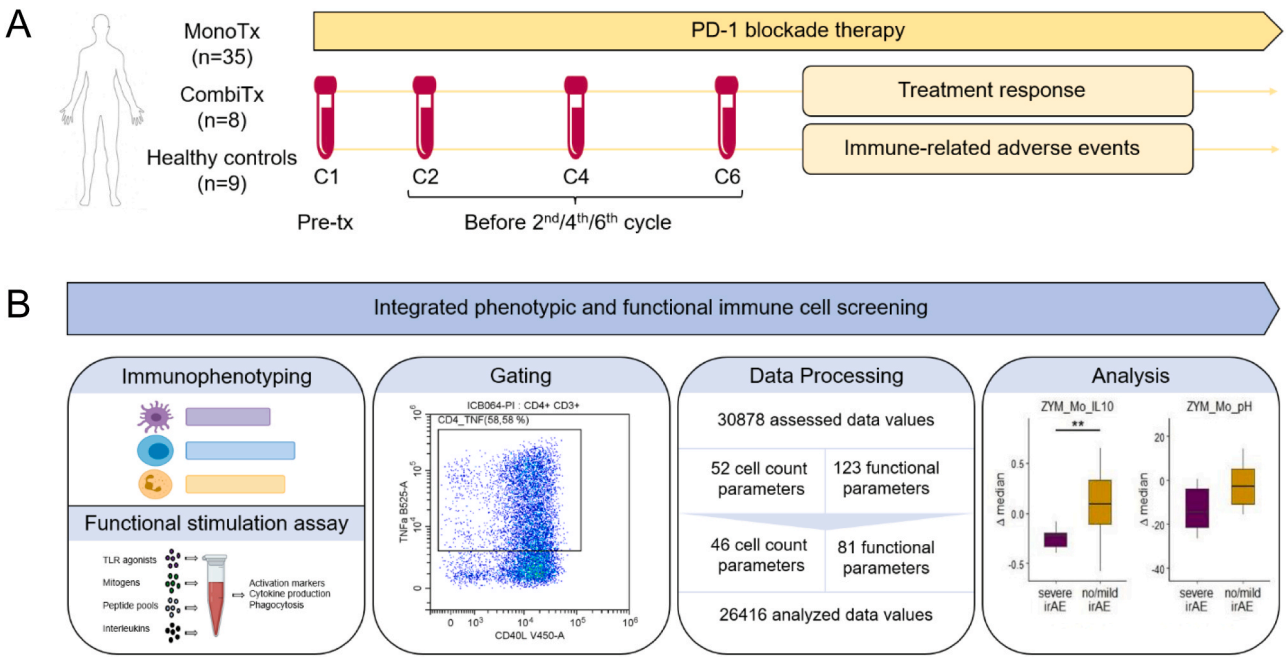

Fig. 1. Study overview. (A) Diagram summarizing the cancer status of the recruited donors and displaying the blood taking and corresponding process for immune cell analysis. (B) Overview of the assessed immune parameters and pipeline for analysis of the flow cytometric data.

comparison between HC and ICB patients implies an already altered immune system in patients prior to ICB initiation.

We grouped patients with stable disease, complete, and partial response into "responders" (R) and patients with progressive disease into "non-responders" (NR) according to iRECIST [19] and clinical assessment by the initial staging upon ICB initiation. No parameter showed a significant difference between responders and non-responders at baseline (Fig. S6). Considering the clinical significance of severe and life-threatening irAE, we divided our patient cohort into patients affected by severe irAE (s-irAE) defined as CTCAE grade > 2 requiring at least temporary ICB treatment discontinuation and systemic immunosuppressive treatment, patients affected by no irAE or only mild irAE defined as CTCAE grade 1–2. Notably, in a similar baseline patient analysis with patients grouped according to the occurrence of s-irAE, we observed a tendency towards higher B cell counts, including naïve B cells as well as total B cells, in patients with s-irAE although not reaching statistical significance ($p = 0.06$, $p = 0.07$, respectively) (Fig. S7).

3.3. *Response to ICB is associated with increase in activated T and NK cell subsets and a shift towards IFNγ and TNFα production*

We compared the parameter variation over time between HC and patients undergoing PD1 blockade by retrieving the median relative coefficient of variation of all parameters for each patient (Fig. S4B). ICB patients exhibited on average higher variation compared to HC, particularly those who underwent combination therapy (Figure 2A). Based on the longitudinal variation differences we excluded patients undergoing combination therapy from our further analysis to solely focus on the anti-PD1 antibody-mediated effects. Applying the same approach, we showed that the median variation did not differ between ICB patients according to treatment response, indicating a similar magnitude of PD1-induced changes in the circulating immune cells during ICB with respect to overall variation of the assessed immune parameters (Figure 2B).

To study the underlying immune dynamics during ICB in R versus NR and to reveal how the subsequent application cycles affect immune cells, we utilized the statistical principles of gene set enrichment analysis. By the first follow-up staging upon ICB initiation, 48 % of patients were categorized as R according to clinical assessment and iRECIST criteria [19]. For the enrichment analysis, we first calculated the individual differences of C1 to all other visits, performed a non-parametric statistic based on the classification R versus NR, and then ranked all p values as for enrichment analysis. Instead of gene sets, we grouped the parameters in the elapsed therapy time sets: C2ΔC1, C4ΔC1, C6ΔC1; and subsequently performed enrichment statistics to detect in which therapy period the biggest differences were present (Figure 2C). Hereby, the calculated differences according to response were greatest between pre-treatment (C1) and before the sixth ICB application (C6), indicating effects on circulating immune cells that increase cumulatively with the duration of therapy, rather than, for example, a significant change after the first application.

Different therapy-induced effects between R and NR were observed in the count as well as in the pooled functional parameters. All significant parameters but one (pooled CD40L-stimulated B cells) showed an increase in R compared to NR during the assessed therapy period. Substantial increases in the absolute cell counts were observed mainly in the NK cell compartment (NK bright, total NK, and activated $CD38^+$ NK cells), as well as in two $CD8^+$ T cell subpopulations ($CD8^+$ TEMRA and $CD8^+$ $CD28^-$), which widely embody the same type of $CD8^+$ T cells measured in two different staining panels (Figure 2D). Both phenotypes are associated with either functional exhaustion or recent *in vivo* activation and differentiation into effector T cells, with both explanations being conceivable under ICB. However, our functional analysis also revealed a substantial increase in IFNγ and TNFα production by $CD8^+$ T cells in R (Figure 2E), which would strongly support the notion that these cells are not exhausted but rather freshly *in vivo* differentiated effector T cells. Consistent with the quantitative and qualitative changes in the $CD8^+$ T cell compartment, we also detected an increased NK cell-derived IFNγ as well as a generally higher responsiveness of NK cells towards the TLR agonist R848 in R. In addition, $CD4^+$ T cell-derived TNFα in R was significantly increased, which together with the elevated TNFα level by $CD8^+$ T cells may contribute to higher TNFα-associated T cell-mediated anti-cancer responses that are associated with enhanced efficacy of immunotherapies [20].

Overall, the results of our *ex vivo* assessment of the reactivity and functional qualities of peripheral immune cells of ICB-treated patients

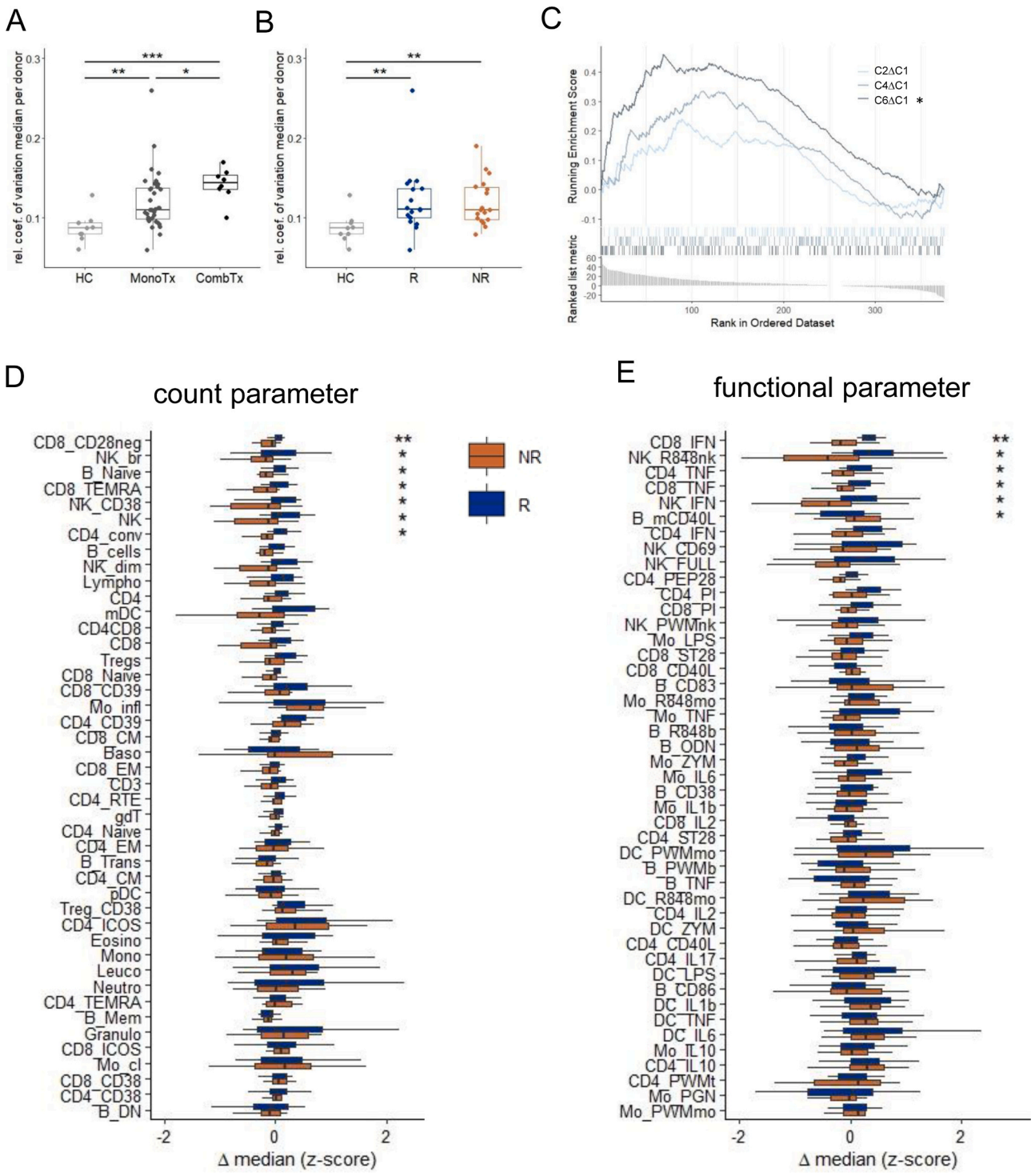

Fig. 2. Immune dynamics during PD1 blockade therapy in responding (R) versus non-responding (NR) patients. (A) The average variation across all parameters during the assessed time period was compared between healthy controls (HC, n = 9) and cancer patients treated with anti-PD1 antibodies alone (MonoTx, n = 35) and patients receiving PD1 blockade therapy in combination with other anti-cancer treatments (CombTx, n = 8). (B) Comparison of parameter variation during MonoTx based on therapy response. (C) "Gene" set enrichment plots adapted to display the enrichment of differences over therapy time between R (n = 17) and NR (n = 18) patients. The p values were obtained by non-parametric comparison of all delta-values of C2, C4, and C6 to C1 of each individual parameters between the two patient grouping. (D-E) Box-Whisker-Plots of all count parameters and (D) all pooled functional parameters comparing R and NR (E) are displayed. Statistical analysis: (A-B) Kruskal-Wallis test with Dunn's multiple comparisons post-hoc test and Benjamini-Hochberg p value adjustment; (C) Kolmogorow-Smirnow test with Benjamini-Hochberg p value adjustment due to multiple comparisons (D-E) Mann-Whitney test; $p < 0.05$ = *, $p < 0.01$ = ** , $p < 0.001$ = ** *.

complement the common view that ICB treatment results in rejuvenation of an antitumor response mediated in particular by activated T and also NK cells.

3.4. Severe irAE are associated with increase in activated CD8$^+$ and CD4$^+$ T cell subsets and decreased IL10 production by monocytes upon stimulation

By applying the same approach, we analyzed the immune profile differences related to s-irAE, defined as CTCAE grade > 2 requiring ICB discontinuation and application of immunosuppressive treatment (n = 6), by comparing these patients and those who did not develop irAE (n = 24) or only developed mild irAE with CTCAE grade 1–2 (n = 5) (Tab. S4). Using our adapted parameter enrichment analysis, as described above, the largest differences between s-irAE and no/mild irAE patients were analogously detected at C6 (Figure 3B). In all affected patients, s-irAE occurred after the last immunological assessment.

Next, we compared the count and pooled functional parameters between s-irAE and no/mild irAE patients via standard univariate analysis. The top four significant count parameters were CD8$^+$ T cell subpopulations including effector (CD8$^+$ TEMRA and CD8$^+$ CD28$^-$), activated (CD39$^+$), and effector memory like CD8$^+$ T cells (Figure 3C). The significantly higher increase of activated T cells in patients affected by s-irAE compared to no/mild irAE was also detectable in the subset of CD39$^+$ CD4$^+$ T cells. A tendency towards a similar simultaneous increase of related effector differentiated CD4$^+$ T cell subsets was also noticeable, although insignificant (CD4$^+$ EM, p = 0.06; CD4$^+$ TEMRA, p = 0.09). In addition, an increase of NK cells and their related subpopulations (dim and bright NK cells) was detected in s-irAE-affected patients. A further detailed comparison of the statistically significant count parameters between the subgroups of patients with severe/mild/no irAE showed a higher immunological similarity between the patients with no and only mild irAE (Fig. S8) supporting our decision to focus on the clinically more relevant cohort of patients affected by s-irAE. In contrast to our analysis regarding treatment response, no significant parallel increase in the related functional parameters of NK (IFNγ) and T cells (TNFα, IFNγ) was detected in irAE patients (Figure 3D), but instead more IL17A-expressing CD4$^+$ T cells paralleled the expansion of CD4$^+$ T cells. Significance was not reached, however IL17A-expressing CD4$^+$ T cells have been already described as a relevant mediator for irAE [21–23]. The only significantly different pooled functional parameter between s-irAE and no/mild irAE was the increased responsiveness of monocytes to zymosan-mediated stimulation in no/mild irAE patients. The same trend of increased monocytic responsiveness to zymosan was detectable in all related single functional parameters (Figure 3E). In particular, IL10 expression upon zymosan stimulation was significantly lower in patients with s-irAE compared to patients with no/mild irAE. Considering the lower production of IL10 by monocytes and the observed increase in activated T cell subsets in the irAE-affected patient cohort as well as the immunosuppressive role of IL10, we hypothesized that the diminished IL10 production by monocytes may result in excessive and uncontrolled expansion of activated T cells including irAE-inducing, autoreactive, and possibly IL17A-expressing T cells.

3.5. Monocyte-derived IL10 inhibits T cell proliferation

Due to the described significantly lower expression of IL10 by monocytes upon stimulation among patients with s-irAE compared to no/mild irAE patients, we wanted to study in more detail this novel effect of ICB treatment. Since zymosan is known to bind to TLR2/6 as well as to Dectin-1 [24], we assumed that in the context of ICB treatment instead of zymosan, endogenous ligands of both receptors may provoke increased IL10 expression that should be detectable in the patients IL10 serum levels. Consistent with this assumption, serum IL10 levels increased during ICB in no/mild irAE patients, whereas patients with s-irAE lacked this IL10 rise (Figure 4A). This difference is thus in line with the presented functional data regarding the *ex vivo* stimulated monocytes (Figure 3D). Furthermore, serum IL10 levels correlated negatively with CD8$^+$ T cell expansion dynamics during therapy in ICB patients, supporting the idea that IL10 expression by monocytes co-controls T cell expansion during ICB treatment, with high IL10 levels keeping autoreactive T cells in check and suppressing irAE development (Figure 4B). To further underline that monocyte-derived IL10 contribute to the observed IL10 serum level differences between s-irAE and no/mild irAE patients, we cytometrically enriched monocytes and assessed the monocytic IL10 production in the supernatant after 24 h culture. Consistent with the different IL10 serum levels we also measured higher IL10 levels in the supernatant of monocytes from no/mild irAE compared to s-irAE patients (Figure 4C). Notably, IL10 is known to be a crucial factor for T cell expansion in T cells [25,26]. Finally, to demonstrate that IL10 alone can significantly influence the proliferation of antigen-specific T cells and could therefore be responsible for the increased T cell expansion observed in patients with s-irAE in our study, we stimulated autologous patient-derived T cells with a peptide pool mix containing peptide antigens from various pathogens in the presence or absence of monocytic supernatant impacting proliferation of CFSE-labeled T cells (Figure 4D). Addition of monocytic supernatant from patients with no/mild irAE - containing significantly more IL10 than supernatants from s-irAE-affected patients as seen in Figure 4C - strongly inhibited the T cell proliferation with a drop from 19.5 % to 8.1 %. In contrast, the supernatant derived from patients with s-irAE did not show any effect on the T cell proliferation.

This evidence supports our previously formulated hypothesis that monocyte-derived IL10 is a critical factor in the control and inhibition of T cell expansion, particularly of IL17A-producing autoreactive T cells (Figure 4E), in the context of ICB treatment.

4. Discussion

Longitudinal analysis of therapy-induced dynamics and shifts of phenotypes and functions in immune cells is essential for a deeper mechanistic understanding of ICB allowing an assessment detached from inter-individual immune variances.

The comparison between R and NR patients revealed a disparate pattern of IFNγ and TNFα production by CD8$^+$, CD4$^+$, and NK cells after stimulation, with an increase in R patients during therapy. These elevated cytokine levels in R support the concept that PD1 blockade rejuvenates T cell responses, especially those of CD8$^+$ T cells [27,28]. Our data also suggest that the reinvigoration/activation of CD4$^+$ T and NK cells and their subsequent production of IFNγ and TNFα may additionally be decisive for the response to treatment. Our assumption is supported by other studies, which consider these populations as major players in the context of immunotherapies [29–32]. Although both cytokines can promote tumorigenesis under certain circumstances, an increase of IFNγ and TNFα levels in the TME as well as in the periphery has been reported as positive prognostic factors in two studies, which can be linked with the observed increase of these effector molecules in T and NK cells [20, 33, 34]. Besides this elevated cytokine production, we further detected significant corresponding increases of the absolute count of conventional CD4$^+$ T cells (excluding Tregs) and NK cells as well as CD28$^-$ CD8$^+$ T cells and TEMRA CD8$^+$ T cells in R. This suggests that the functional shifts observed in R, are at least partly explained by the expansion of the specific populations. Although CD28$^-$ CD8$^+$ and TEMRA CD8$^+$ T cells are often associated with an exhausted T cell status, these phenotypes can also be displayed by recently activated and proliferating T cells, often referred to as effector T cells, which would also explain the detected increase of the antitumor effector cytokines IFNγ and TNFα among T cells [35,36]. Based on our explorative data, we propose that dynamic immune changes that occur early on during ICB, may be a promising predictive marker for treatment response, although this needs to be validated in a larger and more homogeneous cohort regarding tumor entities and taking into account variables e.g., prior treatment regimens and individual risk factors.

We further observed a pronounced increase in the frequency of effector lymphocyte subsets such as CD8$^+$ T cells, activated CD4$^+$ T cells (in particular CD39$^+$ CD4$^+$ T cells), and NK cells in patients with s-irAE

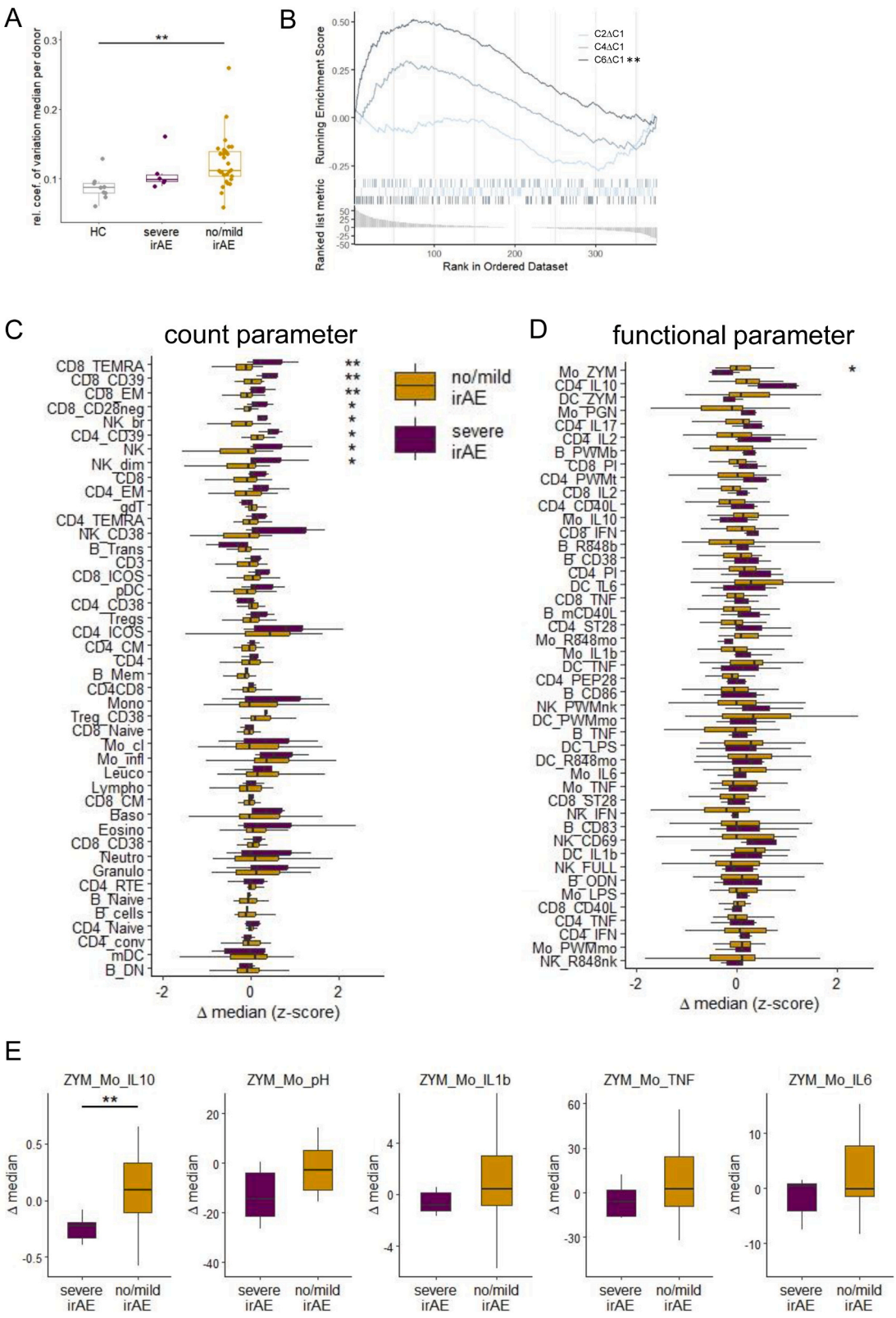

Fig. 3. Immune dynamics during PD1 blockade therapy in patients with severe vs. no/mild irAE. (A) The average variation across all parameters during the assessed time period was compared between healthy controls (HC, n = 9), patients with severe (n = 6) and no/mild (n = 29) irAE treated with anti-PD1 antibodies alone. (B) "Gene" set enrichment plots adapted to display the enrichment of differences over therapy time between patients with severe and no/mild irAE. The p values were obtained by non-parametric comparison of all delta-values of C2, C4, and C6 to C1 of each individual parameters between the two patient groups (C-D) Box-Whisker-Plots of all count parameters and (C) all pooled functional parameters comparing severe irAE and no/mild irAE (D) are displayed. (E) Box-Whisker plots of all single functional parameter divided into patients with severe irAE and no/mild irAE contributing to the Mo-ZYM pooled parameter. Statistical analysis: (A) Kruskal-Wallis test with Dunn's multiple comparisons post-hoc test and Benjamini-Hochberg p value adjustment; (B) Kolmogorow-Smirnow test with Benjamini-Hochberg p value adjustment due to multiple comparisons (C-E) Mann-Whitney test; $p < 0.05$ = *, $p < 0.01$ = ** , $p < 0.001$ = ** *.

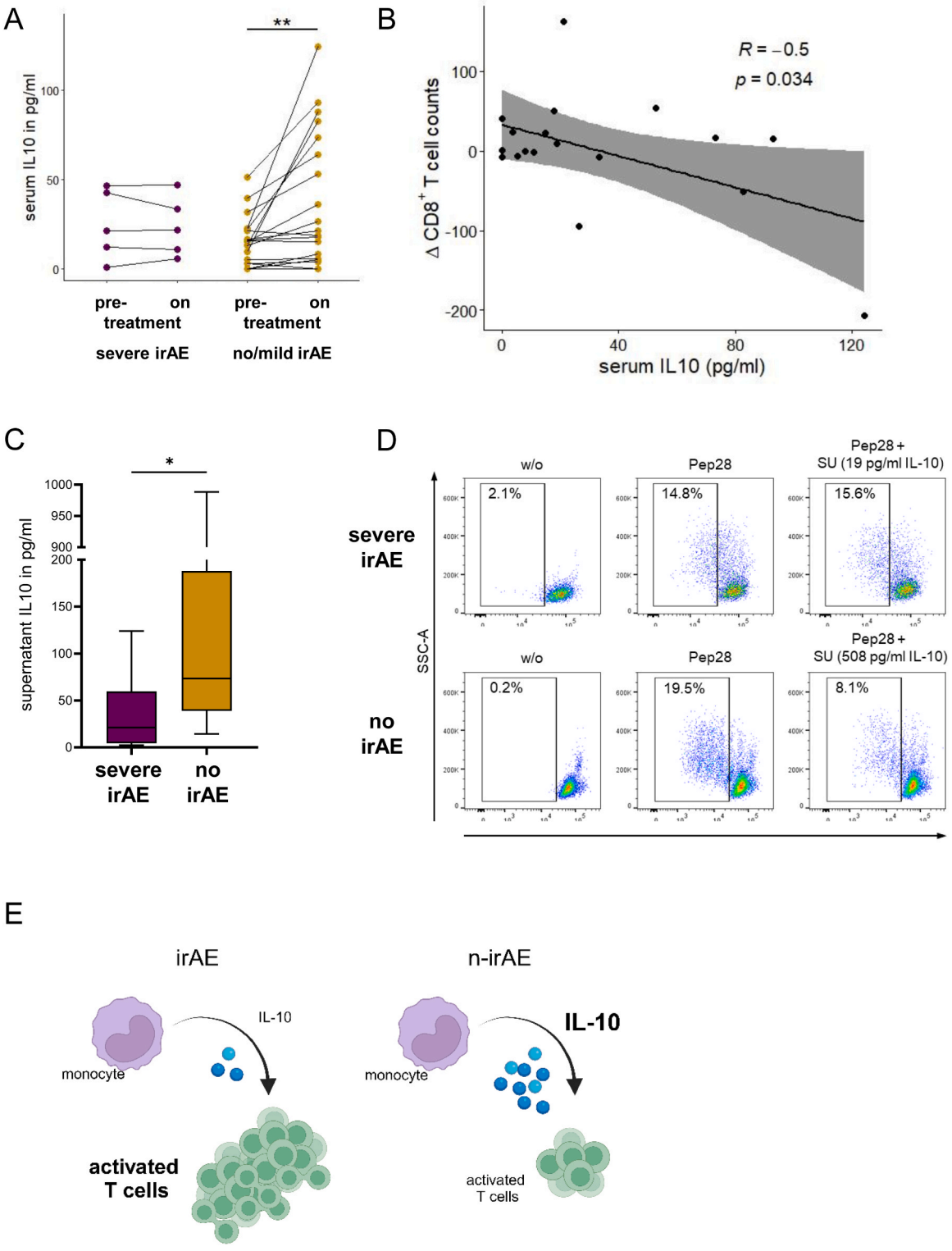

Fig. 4. Differences in the expression of IL10 by monocytes among ICB patients affect T cell expansion. (A) Side by side comparison of changes in the IL10 serum levels in available samples during therapy between severe irAE (n = 5, due to missing C1 serum sample from patient ICB004) and no/mild irAE patients (n = 19) displayed as paired dot-plot. (B) The relation of IL10 serum levels versus the change of $CD8^+$ T cell counts upon treatment shown as a scatter plot (n = 17). (C) The Whisker-Box plot summarizes the IL10 secretion of monocytes from severe vs. no/mild irAE patients measured after 24 h cultivation in the supernatant by ELISA. (D) Peptide stimulated and CFSE-labelled T cells of ICB treated patients were flow cytometrically measured after 4 days. The dot-plots show the CFSE-labeling of $CD3^+CD8^+CD4^-$ gated lymphocytes from one representative s-irAE and no/mild irAE patient (n = 3). IL10 concentration in the supernatant of the added monocyte cultures are indicated above the respective plot.(E) Graphical summary created with BioRender.com of the hypothesis how differences in monocyte-derived IL10 influence irAE development. Statistical analysis: (A) Wilcoxon signed rank test (B) spearman correlation (C) Mann-Whitney test; $p < 0.05 = *$, $p < 0.01 = **$.

compared to no/mild irAE. This effect was independent of therapy response. Remarkably, the pronounced effector lymphocyte increase surpassed the magnitude of the analogous increase observed in R. Based on the wide spectrum of ICB-induced inflammatory adverse events, the pathogenesis of irAE is likely to be multifactorial, but the currently predominant explanatory paradigm focuses on T as well as B cell-mediated autoimmune processes [37,38]. Notably, the observed differences between R and NR regarding the effector cytokines IFNγ and TNFα were not prominent in the irAE comparison. However, we found a tendency towards higher production of the autoimmune- and irAE-associated cytokine IL17A upon stimulation of $CD4^+$ T cells in patients affected by s-irAE compared to no/mild irAE, although not significant. Although statistically not significant, we observed a tendency towards an increased number of effector memory $CD4^+$ T cells in patients affected by s-irAE.

Furthermore, the analysis of s-irAE vs. no/mild irAE patients also elucidated a general ICB-induced increase in the responsiveness of monocytes to a TLR2/6- and dectin-1-dependent zymosan stimulation, which was absent in patients affected by s-irAE. Several endogenous TLR2 ligands (e.g., HMGB1, HSP60, HSP70) have already been described to be elevated in cancer patients [39–41] and together with PD1 blockade may result in activated monocytes that enhance lymphocyte-mediated antitumor responses and/or off-tumor autoimmune inflammation processes leading to irAE. Our data revealed in particular that IL10 expression in monocytes was diminished in s-irAE patients during ongoing ICB treatment, with IL10 known to be able to reduce T cell proliferation [25, 26, 42]. The presented data regarding the higher IL10 serum levels in no/mild irAE patients as well as the higher supernatant IL10 levels from monocytes derived from these patients compared to patients affected by s-irAE further support the hypothesis that the IL10 production by monocytes could be relevant to the prevention of irAE onset. Additionally, we observed a moderate negative correlation of $CD8^+$ T cell expansion and IL10 serum levels. The same inverse relationship we also found for IL10 and the T cell subsets that were different between s-irAE and no/mild irAE (Figure 3C), e.g. activated ($CD39^+$), effector ($CD8^+$ TEMRA and $CD8^+$ CD28) and effector memory like $CD8^+$ T cells, $CD39^+$ $CD4^+$ T cells, but probably due to higher variance in these smaller subsets compared to total $CD8^+$ T cell counts the correlations were not significant with the exception of $CD39^+$ $CD4^+$ T cell expansion and serum IL10 (data not shown). We further confirmed through *in vitro* proliferation experiments that the differences of IL10 production by monocytes from s-irAE and no/mild irAE patients can impact the antigen-driven expansion of T cells. Moreover, in line with the observed decrease of IL10 production by monocytes in patients with s-irAE and trend towards an increase of IL17A-expressing T cells, several other studies could show that IL10 has a strong impact on IL17A expression by T cells, which are generally seen as one of the main pathological drivers in autoreactive adaptive immune responses as Tc17 cells in multiples sclerosis [43] or Th17 cells in psoriasis [44] and as reported in ICB patients suffering from irAE [21, 22, 42]. Although we could confirm with patient material that monocytes-derived IL10 affects T cell proliferation, its direct effect on the promotion of autoreactive and IL17A-expressing T cells has to be proved in future studies. Baseline IL10 levels in patients undergoing ICB treatment were further shown to be correlated with irAE occurrence in two retrospective studies [45,46]. However, to our knowledge, the impact of monocyte-derived IL10 during ICB therapy on irAE development has not been reported yet and is adding to the concept that ICB affects the innate immune system in a way that may be crucial to the clinical outcome of patients in terms of toxicities [13, 14, 16].

The patient cohort size of our study was limited due to the dependence of the reported functional assays on fresh blood samples, with 17 stimulations being performed in parallel per patient and time point. Nevertheless, we were able to include 43 patients in this prospective study and conduct pre- and on-treatment whole blood analyses resulting in the collection of more than 30,000 cytometric data values. Using fresh samples allowed us to keep stimulation conditions as physiological as possible as well as to avoid freezing and thawing procedures, which are known to result in distorted and biased outcomes especially regarding monocytic effector functions [47–49]. The prospective character of the study further did not allow a more balanced patient distribution regarding treatment response and toxicity. The patient population studied here represents a heterogenous cohort regarding tumor entities as well as prior treatment regimens and individual risk factors. A further disbalance can be observed in the sex distribution of our patient cohort. We did not perform adjustment for multiple testing with the goal of avoiding higher risk for false negatives (type II errors). This led to the deliberate acceptance of an increased risk for false positives (type I errors). Our study primarily focused on s-irAE development due to its profound and direct clinical relevance. Although frequent, mild irAE do not require ICB discontinuation or systemic immunosuppressive treatment, thus largely making them irrelevant regarding the patient's prognosis – in stark contrast to s-irAE. The limited sample size of our study additionally constrained our ability to investigate the association between immunological signatures and organ-specific irAE affection.

5. Conclusion

In summary, our explorative study combining phenotypic and functional analyses allowed a holistic system-wide examination of PD1 blockade-induced dynamic immune alterations and revealed expected as well as novel effects of ICB on circulating immune cell populations, which shed additional light on the mechanisms of action of PD1 blockade as well as the associated mechanisms behind PD1 blockade-induced autotoxicity. Our data underpin the association between circulating monocytes and the pathogenesis of s-irAE by showing a novel mechanism based on reduced monocytic IL10 expression in the context of s-irAE as part of a complex multifactorial immunological process. Since cohort-specific immune changes occurred only as therapy progressed, our data also highlight the importance of longitudinal immune monitoring of patients undergoing PD1 blockade therapy. Further validation of immune markers associated with treatment response and/or occurrence of severe treatment-related toxicities in larger patient cohorts may thus impact clinical practice and help guide and complement risk stratification of patients undergoing ICB therapy.

Funding

The work was supported by grants from BIH and research funding from Bristol-Myers Squibb (CA209–7FH), Wilhelm-Sander Stiftung (2019.047.1), the Stiftung Charité (BIH Johanna Quandt funding), and the Deutsche Forschungsgemeinschaft (NA 950/5–1). S. R. received doctoral scholarship from the Berlin Cancer Society (Berliner Krebsgesellschaft e.V.) for his work on this project. S. K. was funded by the Berlin School of Integrative Oncology (BSIO). F. W. is participant in the BIH-Charité Clinician Scientist Program funded by the Charité-Universitätsmedizin Berlin and the Berlin Institute of Health.

CRediT authorship contribution statement

Stanislav Rosnev: Conceptualization, Funding acquisition, Project administration, Investigation, Writing - original draft. Baldur Sterner: Investigation, Resources. **Phillip Schiele:** Investigation. **Stefan Kolling:** Investigation. **Markus Martin:** Investigation. Anne Flörcken: Resources. **Barbara Erber:** Resources. **Friedrich Wittenbecher:** Resources. **Grzegorz Kofla:** Resources. **Annika Kurreck:** Resources. **Tonio Johannes Lukas Lang:** Resources. **Jobst C. von Einem:** Resources. **Maria de Santis:** Resources. **Uwe Pelzer:** Resources. **Sebastian Stintzing:** Resources. **Lars Bullinger:** Resources. **Konrad Klinghammer:** Resources. **Dominik Geisel:** Formal analysis, **Sebastian Ochsenreither:** Resources. **Marco Frentsch:** Conceptualization, Formal analysis, Funding acquisition, Project administration,

Supervision, Visualization, Writing – original draft. **Il-Kang Na:** Conceptualization, Funding acquisition, Project administration, Supervision, Writing - review & editing

Declaration of Competing Interest

The authors declare that they have no competing financial interests. IKN receives research funding from BMS and - unrelated to this study - further research funding from Shire/Takeda, Sangamo Therapeutics, Octapharma and Novartis. SS receives honoraria for talks, advisory board role and travel support from Astra-Zeneca, Bayer, BMS, ESAI, Lilly, Merck KGaA, MSD, Pierre-Fabre, Roche, Sanofi, Servier, Taiho, Takeda, and funding of scientific projects from Merck KGaA, Pierre-Fabre, Servier, and Roche. MS receives honoraria for lectures, advisory boards, consultancy and travel expenses from AAA, Amgen, Astellas, AstraZeneca, Basilea, Bayer, Bioclin, BMS, EISAI, Exelixis, Ferring, Immunomedics, Ipsen, Janssen, MSD, Merck, Novartis, Pfizer, Pierre Fabre, Roche, Sandoz, Sanofi, SeaGen, and Takeda. AF receives honoraria and travel expenses from PharmaMar and Ipsen.JCvE receives honoraria for talks, advisory board role and travel support from Astra-Zeneca, BMS, ESAI, Lilly, Bayer, Merck KGaA, MSD, Pierre-Fabre, Roche, Sanofi, Servier, and Taiho.KK reports advisory board participation, invited speaker or conference honoraria from Merck, Sanofi, Merck Sharp & Dohme, Glycotope, Roche, Novartis, and BMS.UP receives honoraria from MSD and AstraZeneca.LB received honoraria from Seattle Genetics, Sanofi, Astellas, Amgen, consultancy fee from Gilead, Hexal, and Menarini, consultancy fee and Honoraria Abbvie, BMS/Celgene, Daiichi Sankyo, Janssen, Jazz Pharmaceuticals, Novartis and Pfizer, and research funding from Bayer and Jazz Pharmaceuticals.

Appendix A. Supporting information

Supplementary data associated with this article can be found in the online version at doi:10.1016/j.ejca.2025.115252.

Data availability statement

All data needed to evaluate the conclusions in the paper are present in the paper and the Supplementary Materials. Raw data will be made available on request.

References

[1] Vaddepally RK, Kharel P, Pandey R, Garje R, Chandra AB. Review of indications of FDA-approved immune checkpoint inhibitors per NCCN guidelines with the level of evidence. Cancers 2020;12(3):738.

[2] Pons-Tostivint E, Latouche A, Vaflard P, et al. Comparative analysis of durable responses on immune checkpoint inhibitors versus other systemic therapies: a pooled analysis of phase III trials. JCO Precis Oncol 2019;(3):1–10. https://doi.org/10.1200/PO.18.00114.

[3] Jenkins RW, Barbie DA, Flaherty KT. Mechanisms of resistance to immune checkpoint inhibitors. Br J Cancer 2018;118(1):9–16. https://doi.org/10.1038/bjc.2017.434.

[4] Xu C, Chen YP, Du XJ, et al. Comparative safety of immune checkpoint inhibitors in cancer: systematic review and network meta-analysis. BMJ 2018;363:k4226.

[5] Ramos-Casals M, Brahmer JR, Callahan MK, et al. Immune-related adverse events of checkpoint inhibitors. Published 2020 May 7. Nat Rev Dis Prim 2020;6(1):38. https://doi.org/10.1038/s41572-020-0160-6.

[6] Wang D.Y., Salem J.E., Cohen J.V., et al. Fatal Toxic Effects Associated With Immune Checkpoint Inhibitors: A Systematic Review and Meta-analysis [published correction appears in JAMA Oncol. 2018 Dec 1;4(12):1792]. JAMA Oncol. 2018;4(12):1721-1728. doi:10.1001/jamaoncol.2018.3923.

[7] Spitzer MH, Carmi Y, Reticker-Flynn NE, et al. Systemic immunity is required for effective cancer immunotherapy. Cell 2017;168(3):487–502.e15. https://doi.org/10.1016/j.cell.2016.12.022.

[8] Hiam-Galvez KJ, Allen BM, Spitzer MH. Systemic immunity in cancer. Nat Rev Cancer 2021;21(6):345–59. https://doi.org/10.1038/s41568-021-00347-z.

[9] Wherry EJ, Kurachi M. Molecular and cellular insights into T cell exhaustion. Nat Rev Immunol 2015;15(8):486–99. https://doi.org/10.1038/nri3862.

[10] Yost KE, Satpathy AT, Wells DK, et al. Clonal replacement of tumor-specific T cells following PD-1 blockade. Nat Med 2019;25(8):1251–9. https://doi.org/10.1038/s41591-019-0522-3.

[11] Wu TD, Madireddi S, de Almeida PE, et al. Peripheral T cell expansion predicts tumour infiltration and clinical response. Nature 2020;579(7798):274–8. https://doi.org/10.1038/s41586-020-2056-8.

[12] Zhang J, Ji Z, Caushi JX, et al. Compartmental analysis of T-cell clonal dynamics as a function of pathologic response to neoadjuvant PD-1 blockade in resectable non-small cell lung cancer. Clin Cancer Res 2020;26(6):1327–37. https://doi.org/10.1158/1078-0432.CCR-19-2931.

[13] Oh SA, Wu DC, Cheung J, et al. PD-L1 expression by dendritic cells is a key regulator of T-cell immunity in cancer. Nat Cancer 2020;1(7):681–91. https://doi.org/10.1038/s43018-020-0075-x.

[14] Mayoux M, Roller A, Pulko V, et al. Dendritic cells dictate responses to PD-L1 blockade cancer immunotherapy [published correction appears in. eaav7431 Sci Transl Med 2020;12(534):546. https://doi.org/10.1126/scitranslmed.aav7431.

[15] Strauss L, Mahmoud MAA, Weaver JD, et al. Targeted deletion of PD-1 in myeloid cells induces antitumor immunity. Sci Immunol 2020;5(43):eaay1863. https://doi.org/10.1126/sciimmunol.aay1863.

[16] Sun J, Schiffman J, Raghunath A, Ng Tang D, Chen H, Sharma P. Concurrent decrease in IL-10 with development of immune-related adverse events in a patient treated with anti-CTLA-4 therapy. Cancer Immun 2008;8(9). Published 2008 May 27.

[17] Nuñez NG, Berner F, Friebel E, et al. Immune signatures predict development of autoimmune toxicity in patients with cancer treated with immune checkpoint inhibitors. Med 2023;4(2):113–129.e7. https://doi.org/10.1016/j.medj.2022.12.007.

[18] Seymour L, Bogaerts J, Perrone A, et al. iRECIST: guidelines for response criteria for use in trials testing immunotherapeutics [published correction appears in Lancet Oncol. 2019 May;20(5):e242]. Lancet Oncol 2017;18(3):e143–52. https://doi.org/10.1016/S1470-2045(17)30074-8.

[19] Bender R, Lange S. Adjusting for multiple testing–when and how? J Clin Epidemiol 2001;54(4):343–9. https://doi.org/10.1016/s0895-4356(00)00314-0.

[20] Vredevoogd DW, Kuilman T, Ligtenberg MA, et al. Augmenting immunotherapy impact by lowering tumor TNF cytotoxicity threshold [published correction appears in Cell. 2020 Jan 23;180(2):404-405]. Cell 2019;178(3):585–599.e15. https://doi.org/10.1016/j.cell.2019.06.014.

[21] Lechner MG, Cheng MI, Patel AY, et al. Inhibition of IL-17A protects against thyroid immune-related adverse events while preserving checkpoint inhibitor antitumor efficacy. J Immunol 2022;209(4):696–709. https://doi.org/10.4049/jimmunol.2200244.

[22] Mazzarella L, Giugliano S, D'Amico P, et al. Evidence for interleukin 17 involvement in severe immune-related neuroendocrine toxicity. Eur J Cancer 2020;141:218–24. https://doi.org/10.1016/j.ejca.2020.10.006.

[23] Tyan K, Baginska J, Brainard M, et al. Cytokine changes during immune-related adverse events and corticosteroid treatment in melanoma patients receiving immune checkpoint inhibitors. Cancer Immunol Immunother 2021;70(8):2209–21. https://doi.org/10.1007/s00262-021-02855-1.

[24] Dillon S, Agrawal S, Banerjee K, et al. Yeast zymosan, a stimulus for TLR2 and dectin-1, induces regulatory antigen-presenting cells and immunological tolerance. J Clin Invest 2006;116(4):916–28. https://doi.org/10.1172/JCI27203.

[25] Akdis CA, Blaser K. Mechanisms of interleukin-10-mediated immune suppression. Immunology 2001;103(2):131–6. https://doi.org/10.1046/j.1365-2567.2001.01235.x.

[26] Smith LK, Boukhaled GM, Condotta SA, et al. Interleukin-10 directly inhibits $CD8^+$ T cell function by enhancing N-glycan branching to decrease antigen sensitivity. Immunity 2018;48(2):299–312.e5. https://doi.org/10.1016/j.immuni.2018.01.006.

[27] Centanni M, Moes DJAR, Trocóniz IF, Ciccolini J, van Hasselt JGC. Clinical pharmacokinetics and pharmacodynamics of immune checkpoint inhibitors. Clin Pharm 2019;58(7):835–57. https://doi.org/10.1007/s40262-019-00748-2.

[28] Huang AC, Postow MA, Orlowski RJ, et al. T-cell invigoration to tumour burden ratio associated with anti-PD-1 response. Nature 2017;545(7652):60–5. https://doi.org/10.1038/nature22079.

[29] Kim KH, Cho J, Ku BM, et al. The first-week proliferative response of peripheral blood PD-1^+CD8^+ T cells predicts the response to anti-PD-1 therapy in solid tumors [published correction appears in Clin Cancer Res. 2020 Dec 15;26(24):6610]. Clin Cancer Res 2019;25(7):2144–54. https://doi.org/10.1158/1078-0432.CCR-18-1449.

[30] Borst J, Ahrends T, Bąbała N, Melief CJM, Kastenmüller W. $CD4^+$ T cell help in cancer immunology and immunotherapy. Nat Rev Immunol 2018;18(10):635–47. https://doi.org/10.1038/s41577-018-0044-0.

[31] Hsu J, Hodgins JJ, Marathe M, et al. Contribution of NK cells to immunotherapy mediated by PD-1/PD-L1 blockade. J Clin Invest 2018;128(10):4654–68. https://doi.org/10.1172/JCI99317.

[32] Parker BS, Rautela J, Hertzog PJ. Antitumour actions of interferons: implications for cancer therapy. Nat Rev Cancer 2016;16(3):131–44. https://doi.org/10.1038/nrc.2016.14.

[33] Montfort A, Colacios C, Levade T, Andrieu-Abadie N, Meyer N, Ségui B. The TNF paradox in cancer progression and immunotherapy [published correction appears in Front Immunol. 2019 Oct 22;10:2515]. Published 2019 Jul 31 Front Immunol 2019;10:1818. https://doi.org/10.3389/fimmu.2019.01818.

[34] Grasso CS, Tsoi J, Onyshchenko M, et al. Conserved interferon-γ signaling drives clinical response to immune checkpoint blockade therapy in melanoma [published correction appears in Cancer Cell. 2021 Jan 11;39(1):122]. Cancer Cell 2020;38(4):500–515.e3. https://doi.org/10.1016/j.ccell.2020.08.005.

[35] Lo DJ, Weaver TA, Stempora L, et al. Selective targeting of human alloresponsive CD8+ effector memory T cells based on CD2 expression. Am J Transpl 2011;11(1):22–33. https://doi.org/10.1111/j.1600-6143.2010.03317.x.

[36] Willinger T, Freeman T, Hasegawa H, McMichael AJ, Callan MF. Molecular signatures distinguish human central memory from effector memory CD8 T cell subsets. J Immunol 2005;175(9):5895–903. https://doi.org/10.4049/jimmunol.175.9.5895.
[37] Sullivan RJ, Weber JS. Immune-related toxicities of checkpoint inhibitors: mechanisms and mitigation strategies. Nat Rev Drug Discov 2022;21(7):495–508. https://doi.org/10.1038/s41573-021-00259-5.
[38] Johnson DB, Balko JM, Compton ML, et al. Fulminant myocarditis with combination immune checkpoint blockade. N Engl J Med 2016;375(18):1749–55. https://doi.org/10.1056/NEJMoa1609214.
[39] Sims GP, Rowe DC, Rietdijk ST, Herbst R, Coyle AJ. HMGB1 and RAGE in inflammation and cancer. Annu Rev Immunol 2010;28:367–88. https://doi.org/10.1146/annurev.immunol.021908.132603.
[40] Wu J, Liu T, Rios Z, Mei Q, Lin X, Cao S. Heat shock proteins and cancer. Trends Pharm Sci 2017;38(3):226–56. https://doi.org/10.1016/j.tips.2016.11.009.
[41] Fucikova J, Moserova I, Urbanova L, et al. Prognostic and predictive value of DAMPs and DAMP-associated processes in cancer. Published 2015 Aug 7 Front Immunol 2015;6:402. https://doi.org/10.3389/fimmu.2015.00402.
[42] Guo B. IL-10 Modulates Th17 pathogenicity during autoimmune diseases. J Clin Cell Immunol 2016;7(2):400. https://doi.org/10.4172/2155-9899.1000400.
[43] Lückel C, Picard F, Raifer H, et al. IL-17^{+} CD8^{+} T cell suppression by dimethyl fumarate associates with clinical response in multiple sclerosis. Published 2019 Dec 16. Nat Commun 2019;10(1):5722. https://doi.org/10.1038/s41467-019-13731-z.
[44] Li B, Huang L, Lv P, et al. The role of Th17 cells in psoriasis. Immunol Res 2020;68(5):296–309. https://doi.org/10.1007/s12026-020-09149-1.
[45] Wang H, Zhou F, Zhao C, et al. Interleukin-10 is a promising marker for immune-related adverse events in patients with non-small cell lung cancer receiving immunotherapy. Front Immunol 2022;13:840313. https://doi.org/10.3389/fimmu.2022.840313.
[46] Phillips GS, Wu J, Hellmann MD, et al. Treatment outcomes of immune-related cutaneous adverse events. J Clin Oncol 2019;37(30):2746–58. https://doi.org/10.1200/JCO.18.02141.
[47] Li B, Yang C, Jia G, et al. Comprehensive evaluation of the effects of long-term cryopreservation on peripheral blood mononuclear cells using flow cytometry. BMC Immunol 2022;23(1):30.
[48] Meijerink M, Ulluwishewa D, Anderson RC, Wells JM. Cryopreservation of monocytes or differentiated immature DCs leads to an altered cytokine response to TLR agonists and microbial stimulation. J Immunol Methods 2011;373(1-2):136–42.
[49] Anderson J, Toh ZQ, Reitsma A, Do LAH, Nathanielsz J, Licciardi PV. Effect of peripheral blood mononuclear cell cryopreservation on innate and adaptive immune responses. J Immunol Methods 2019;465:61–6.